Study on the Flame Retardancy of EVM/Magnesium Hydroxide Composites Optimized with a Flame Retardant Containing Phosphorus and Silicon

Lichun Wang,[1,2] Xinfeng Wu,[1,2] Chao Wu,[1,2] Jinhong Yu,[1,2] Genlin Wang,[1,2] Pingkai Jiang[1,2]

[1]*School of Chemistry and Chemical Engineering, Shanghai Jiao Tong University, Shanghai 200240, People's Republic of China*
[2]*Shanghai Key Lab of Electric Insulation and Thermal Aging, Shanghai Jiao Tong University, Shanghai 200240, People's Republic of China*

Received 4 June 2010; accepted 16 August 2010
DOI 10.1002/app.33226
Published online 16 February 2011 in Wiley Online Library (wileyonlinelibrary.com).

ABSTRACT: A novel phosphorus-silicon-containing flame retardant, spirocyclic pentaerythritol bisphosphorate disphosphoryl chloride/9, 10-dihydro-9-oxa-10-phosphaphanthrene-10-oxide/vinyl methyl dimethoxysilane (SPDV), was synthesized successfully and used for optimizing the flame retardancy of ethylene-vinyl acetate copolymer (EVM) rubber/magnesium hydroxide (MDH) composites. The microstructure of SPDV was characterized and determined by Fourier transform infrared (FTIR) and nuclear magnetic resonance (NMR) spectroscopy. Thermogravimetric analysis (TGA) showed that SPDV had good charring effect in air even at high temperature (800°C). The flame retardancy of the optimized EVM/MDH composites by SPDV was investigated by limiting oxygen index (LOI), cone calorimeter, and UL-94 vertical burning tests. A higher LOI value (29.4%) and better UL-94 rating (V-0) can be achieved for the optimized EVM/MDH composite (EVM-7) than EVM/MDH composite without SPDV (EVM-3) with the total loading of additives. The HRR decreased and residual mass increased gradually as the loading of SPDV increased for the optimized EVM/MDH composites. There existed distinct synergistic intumescent flame-retardant effect between SPDV and MDH in EVM matrix. © 2011 Wiley Periodicals, Inc. J Appl Polym Sci 121: 68–77, 2011

Key words: ethylene-vinyl acetate copolymer; magnesium hydroxide; composites; synthesis; flame retardant

INTRODUCTION

Poly(ethylene-*co*-vinyl acetate) (EVA) was widely used in the wire and cable industry as insulating materials due to its good mechanical and physical properties.[1–3] However, it is easily flammable, and this is why flame retardation of EVA is being widely studied.[4–11] This problem could be solved by using flame-retardant additives, such as halogenated compounds in synergistic combination with antimony trioxide.[12] However, their fire retardant action may be accompanied by negative effects such as generation of corrosive, obscuring, toxic smoke.[13–15] Thus, halogenated flame retardants have been under pressure due to perceived environmental concerns. Moreover, the new regulations like the European Directives on WEEE (Waste of Electric and Electronic Equipment) and RoHS (Restrictions of Hazardous Substances) restrict the demand for some brominated flame retardants. Therefore, there is a growing demand for new, environmental friendly solutions.[15] Many investigations have demonstrated that inorganic hydroxide fillers, such as MDH and aluminum hydroxide (ATH), are excellent nontoxic and smoke-suppressing halogen-free flame-retardant (HFFR) additives.[16–19] They are commonly used for manufacturing HFFR and low smoke cables. These compounds act in both the condensed phase and the gas phase. Their thermal decomposition follows an endothermic reaction to decrease the temperature of materials and releases water into the gas phase to dilute the flame. However, the high loadings required for adequate flame retardant level often lead to difficult processing and deteriorated mechanical properties. Recently, HFFRs composed of two or three elements such as phosphorus, nitrogen, and silicon have been a hot subject of research in flame retardant field. FRs composed of organic phosphaspirobicyclic compounds, which have been investigated by many researchers, and presenting good flame retardancy and excellent char forming ability in many polymeric materials.[20–22] Silicon-containing compounds are considered to be one of the environmental friendly flame retardant materials. Some studies indicate that silicone-containing polymers can improve flame retardancy for many polymer materials.[23–25]

EVM rubber, as a copolymer of ethylene and high content of vinyl acetate, is suitable for use as HFFR

Correspondence to: P. Jiang (pkjiang@sjtu.edu.cn).

wire and cable insulating or sheathing materials because of its good compatibility with inorganic FRs, good resistance to oil and good FR properties. Qu and Li has reported the effects of gamma irradiation on the properties of flame-retardant EVM/MDH blends and found that 60 wt % MDH loading (150 phr) was required to obtain an adequate level of flame retardancy.[26] In this work, the flame retardant SPDV containing phosphorous-silicon was synthesized successfully and used as a charring additive for optimizing the flame retardancy of EVM/MDH composites. Meanwhile, a novel intumescent flame-retardant EVM system had been obtained by the blending of EVM resin, MDH, and SPDV. Its thermal properties and flame retardancy were investigated by TGA, LOI, cone calorimeter, and UL-94 tests. The synergism between MDH and SPDV in EVM matrix was studied; the morphology of the intumescent char layer and its possible mechanism were investigated by scanning electron microscopy (SEM) and FTIR spectroscopy. Finally, the mechanical properties of flame retardant EVM composites were studied.

EXPERIMENTAL

Materials

A commercial cable grade EVM rubber (Levaprene 500HV) was kindly supplied by Bayer Co., Germany. The vinyl acetate content is 50 wt %, the Mooney viscosity (ML_{1+4} (100°C)) is 27 ± 4, MFI (g/10 min) is lower than 5 and the density is 1.00 g/cm^3.

MDH (Magnifin H5IV) with an average particle size of 1.0 μm, the specific surface area of 5.0 m^2/g and coated by amino silane, was supplied by Martinswerk GmbH.

Dialkylated diphenylamine (DDA) was supplied by Taizhou Huangyan Donghai Chemical Co. Ltd, China.

Dicumyl peroxide (DCP) was obtained from Shanghai Gaoqiao Petroleum Co. Ltd, China.

9,10-dihydro-9-oxa-10-phosphaphenanthrene-10-oxide (DOPO) was purchased from Shandong Mingshan Fine Chemical Co. Ltd., China.

Vinylmethyldimethoxy silane (Vmdms; Brand: Silquest A2171) was acquired from GE silicones.

Acetonitrile (CH_3CN), triethylamine, acetone, and pentaerythritol (PER) were acquired from Shanghai Chemical Agent Corp.

Phosphorus oxychloride ($POCl_3$) was purchased from Tingxin Chemical Industry Co. Ltd., China.

Synthesis of SPDV

The first intermediate product spirocyclic pentaerythritol bisphosphorate disphosphoryl chloride (SPDPC) was synthesized successfully through simple dehydrochlorination reaction of PER and $POCl_3$ according to the reported references.[27,28] Instrumental analysis of SPDPC was carried out using FTIR and NMR. FTIR (KBr) (cm^{-1}): 1305 (versus, P[dsbond]O), 1025 (versus, P—O—C), 550 (versus, P—Cl). ^{1}H-NMR (400 MHz, d_6-DMSO, ppm): 4.21–4.24 (d, —CCH_2O—PO—, 8H); ^{31}P NMR (d_6-DMSO, ppm): −6.0–6.3. Another intermediate product 9, 10-dihydro-9-oxa-10-phosphaphenanthrene-10-oxide (DOPO)/vinyl methyl dimethoxy silane (VMDMS) oligomer named as DV was synthesized according to the previous report by Zhong et al.[29] FTIR (KBr) (cm^{-1}): 3421 (Si—OH), 3064 (C—H in phenyl group), 2800–3000 (CH_2, CH_3), 1595 (phenyl group), 1477 (P-phenyl), 1410 (P—CH_2— of aliphatic), 1206 (P=O), 1004–1117 (Si—O—Si), 911 (P—O—phenyl); ^{1}H-NMR (CDCl3, ppm):−0.4–0.1 (Si—CH3), 0.6 (C—CH2—Si), 1.8–1.9 (—CH_2—P), 2.9(—OH); ^{31}P-NMR ($CDCl_3$, ppm): 38–42.

A total of 200 mL acetonitrile, 29.6 g SPDPC (0.1 mol), and 62.2 g DV (0.1 mol) with 0.5 mL triethylamine as catalyst were introduced into a 500-mL three-necked and round-bottomed glass flask with a mechanical stirrer, a thermometer, condenser, and a heating bath. The mixture was stirred for about 4 h at room temperature. Afterwards, the mixture was gradually heated to 90°C and refluxed until no HCl gas was emitted. The reaction would be completed after 10 h at 90°C, when no HCl gas could be detected by the PH value measuring. It was then cooled to room temperature. Finally, the solvent was removed by the vacuum-pumping. The synthesis route for SPDV was shown in Figure 1. The obtained solid was washed three times with acetone. The purified product, a flaxen solid, was obtained (yield: 84%); mp (476.5 to 491.3 K). The microstructure of the synthesized SPDV was characterized by FTIR and NMR spectroscopy shown as Figures 2 and 3, respectively. Number average molecular weight (GPC): 5300. Elem. Anal. Calculated (while $m = 2$): C 49.65%, H 4.49%, O 24.59%, P 14.66%, Si 6.62%. Found: C 49.86%, H 4.63%, O 24.33%, P 14.51%, Si 6.67%.

Preparation of FR-EVM composites

EVM pallets were dried at 40°C in a vacuum for 4 h before processing to remove moisture. Then the EVM-based flame retardant composites were prepared in a Brabender internal mixer at 110°C for 8 min with a speed of 50 rpm. The detailed formulations for EVM rubber and flame retardancy (MDH, SPDV) were shown in Table I. Meanwhile, DCP (2.0 phr) as the crosslinking agent and DDA (0.5 phr) as an antiaging agent were added for each sample. The mixed samples were transferred to a mold and pressed at 175°C for 15 min, and successively cooled to room temperature while maintaining the pressure (12 MPa) to obtain the EVM-based composites sheets for further measurements.

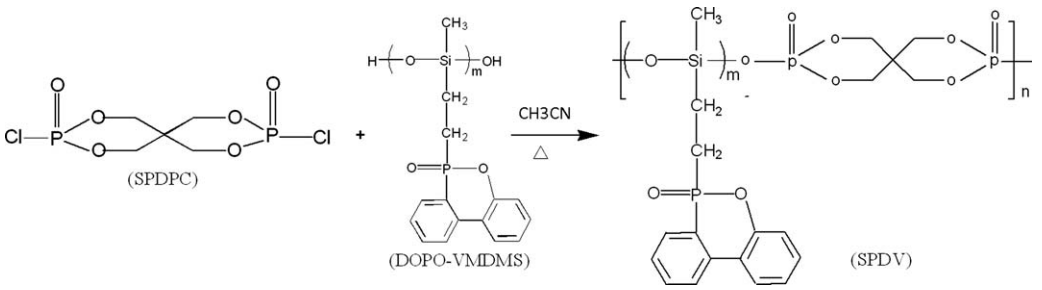

Figure 1 The synthesis route of SPDV.

Measurement and characterization

Characterization of SPDV by FTIR and NMR spectroscopy

The FTIR spectra of SPDV were recorded with KBr powder by using a Perkin–Elmer Paragon 1000 instrument. From Figure 2, it could be observed that absorption of Si—OH (end group in SPDV) and C—H in phenyl group was at about 3427 cm^{-1} and 3074 cm^{-1}, respectively. The peaks at 2800–3000 cm^{-1}, 1596 cm^{-1}, 1478 cm^{-1}, and 1410 cm^{-1} were assigned to the absorption of CH_2 and CH_3 in the branch chain, phenyl group, P-phenyl and CH_2 of spirocycle, and P—CH_2— of aliphatic, respectively. The peaks at 1206 cm^{-1}, 1014–1127 cm^{-1}, and 921 cm^{-1} associated with the stretching mode of P=O, Si—O—Si, P—O—C, and P—O—phenyl, respectively.[23] The structure of SPDV was characterized and determined further by ^{1}H-NMR [Fig. 3(a)] and ^{31}P-NMR [Fig. 3(b)], which were performed on a Mercuryplus 400 (300-MHz) NMR spectrometer with DMSO-d_6 as a solvent. The ^{1}H-NMR spectrum (d_6-DMSO, 400-MHz) of SPDV: the chemical shifts at 7.1–8.3 ppm resulted from the aromatic hydrogens of the biphenol section; the chemical shifts at 4.21–4.24 ppm was from the eight hydrogens of the spirocycle; the chemical shifts at around 1.8–2.1 ppm was assigned to the two hydrogens in —CH_2—P; the chemical shifts at 0.3–0.5 ppm could be assigned to the two hydrogens in C—CH_2—Si; the chemical shifts at about −0.3–0.1 ppm was from the hydrogens of the methyl (Si—CH_3). Moreover, ^{31}P-NMR spectrum (d_6-DMSO, 400-MHz) of SPDV revealed two resonances at 38–42 ppm and −6.5 ppm corresponding to P in phenyl group and P in the spirocycle structure, respectively.

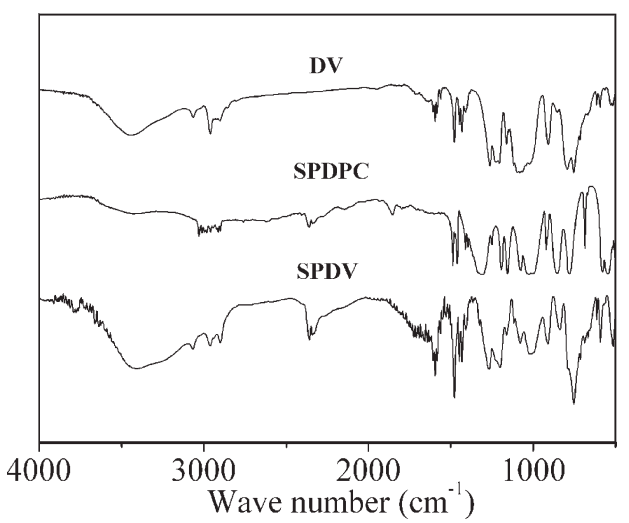

Figure 2 FTIR spectra of DV, SPDPC, and SPDV.

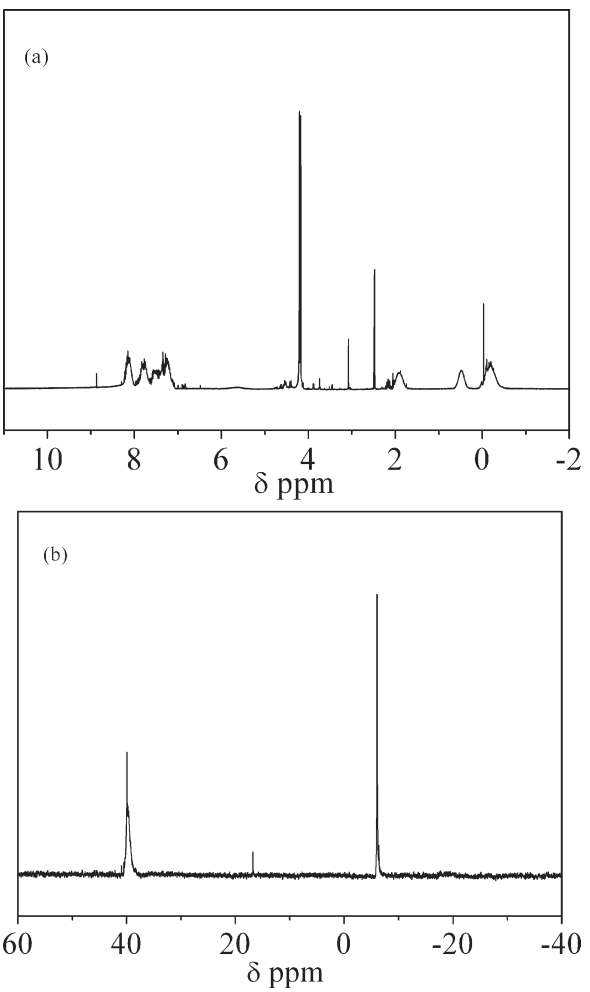

Figure 3 ^{1}H-NMR (a) and ^{31}P-NMR (b) spectra of SPDV in DMSO-d_6.

TABLE I
Flame-Retardant EVM Formulations and the Results of LOI and UL-94 Tests

	Composition of FR-EVM				UL-94		
Code	EVM (phr)	MDH (phr)	SPDV (phr)	LOI (%)	Rate	Ignition time (s)	Drip condition
EVM-1	100	0	0	18.5	No rate	4	Heavy dripping
EVM-2	100	50	0	24.5	No rate	12	Dripping
EVM-3	100	80	0	28.0	No rate	16	Slow dripping
EVM-4	100	120	0	35.5	V-0	28	No dripping
EVM-5	100	50	10	26.3	V-2	15	Slow dripping
EVM-6	100	50	20	27.8	V-0	18	Slow dripping
EVM-7	100	50	30	29.4	V-0	23	No dripping
EVM-8	100	0	30	23.4	V-2	12	Slow dripping

LOI and UL-94 testing of FR-EVM composites

LOI values were measured using an HC-2C type oxygen index instrument (Nanjing Analytical Instrument Factory, China) with the sheets of 130 × 6.5 × 3 mm^3 according to ASTM D 2863-97. The percentage in the O_2-N_2 mixture deemed sufficient to sustain the flame was taken as the LOI value.

UL-94 vertical burning tests were carried out using a vertical burning test instrument (CZF-2 type) (Nanjing Jiangning Analytical Instrument Factory, China) with the sheets of 130 × 13 × 3 mm^3 according to ASTM D 3801.

Cone calorimeter testing of FR-EVM composites

Cone calorimeter tests were carried out in duplicate, using a 35 kW/m^2 incident heat flux, following the procedures indicated in the ISO 5660 standard with a FTT cone calorimeter.[30] Each specimen, of dimensions 100 × 100 × 3 mm^3, was wrapped in aluminum foil and placed on a mineral fiber blanket with the surface level with the holder, such that only the upper face was exposed to the radiant heater. The edge guard was used with all specimens, as was the recommended standard retaining grid to prevent excessive intumescence. The experimental error rate from the cone calorimeter test was about ± 5%. Cone calorimeter technique provides detailed information about ignition behavior, heat release, and smoke evolution during sustained combustion and some key parameters which are correlated well with real fire.[31–33]

Thermogravimetric analysis

Thermogravimetric analysis (TGA) was performed with a Perkin–Elmer Q 50 thermal analyzer at a heating rate of 20°C/min. Samples of 5–10 mg were examined under an air flowing rate of 20 mL/min at the temperatures ranging from room temperature to 800°C.

FTIR spectroscopy analysis of char residue

The FTIR absorption spectra of the FR-EVM composites (the samples of EVM-7 and EVM-8) before combustion and their char residues after combustion in cone calorimeter were characterized with KBr powder by using a Perkin–Elmer Paragon 1000 instrument. The chemical structure of combustion residue was analyzed by FTIR spectra.

Scanning electron microscopy

The morphology analyses of combustion char residues for the FR-EVM composites after cone calorimeter tests were made using a field emission scanning electron microscopy (FE-SEM, JEOL JEM-4701). The gold-coated samples to avoid accumulation of charges were analyzed at an accelerating voltage of 5.0 kV.

Mechanical measurements

The tensile properties of EVM-FR composites were measured on an Instron series IX 4465 material tester at a crosshead speed of 500 mm/min with dumbbell specimens (4 mm wide in the cross section) according to ASTM D 412-06a. All the tests were carried out at 25 ± 2°C.

RESULTS AND DISCUSSION

Flammability of FR-EVM composites

The synthesized flame retardant SPDV containing phosphorous and silicon elements in this work was used as both charring agent and acid source, which was mixed with MDH as gas source and EVM matrix to produce a new intumescent flame-retardant EVM composites. The flame-retardant EVM formulation was summed in Table I. For the investigation of the flame retardancy of flame-retardant EVM composites, LOI values and UL-94vertical burning ratings were tested and the results were listed in Table I in detail. From Table I, it could be found that the LOI values of the EVM/MDH system without SPDV increased as the loading of MDH increased, and the loading of 120 phr MDH was necessary to obtain the V-0 rating in UL-94 tests. The LOI value of EVM/SPDV system without MDH (EVM-8) was only 23.4%, and the UL-94 rating was V-2 because of slow

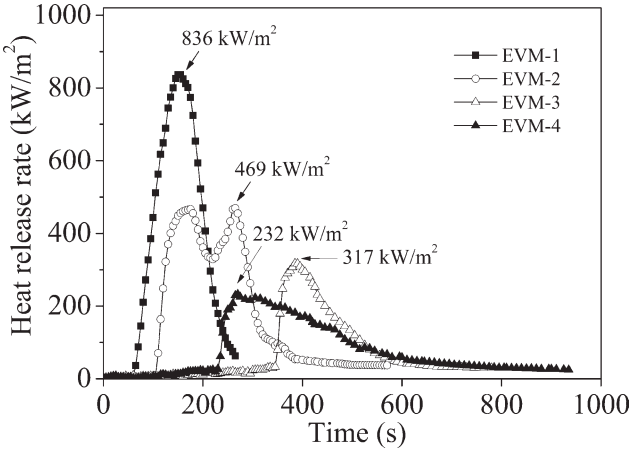

Figure 4 The HRR curves versus burning time for the EVM/MDH systems without SPDV.

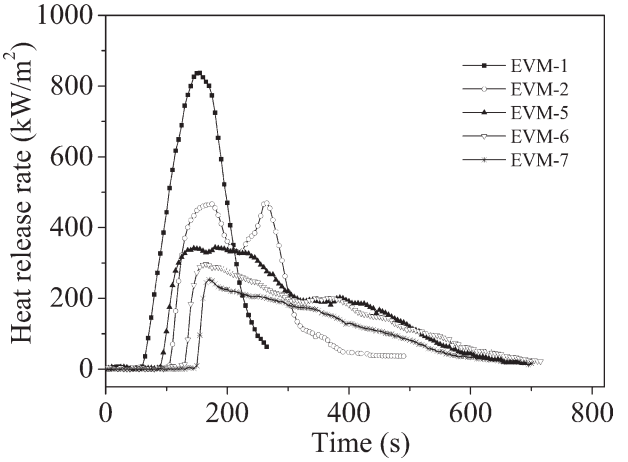

Figure 6 The HRR curves versus burning time for the optimized EVM/MDH composites by SPDV.

dripping. It could be found that the flame retardancy was improved further for the optimized EVM/MDH composites by SPDV. The V-0 rating could be obtained for the optimized flame-retardant EVM system with the loading of 50 phr MDH and 20 phr SPDV (EVM-6). And interestingly, the LOI value for the optimized flame-retardant EVM sample (EVM-7) was 29.4%, which was 1.4% higher than the EVM/MDH sample (EVM-3, LOI = 28.0%) with the same total amount of additives, demonstrating that SPDV had good flame retardant effect on the EVM/MDH systems and a significant synergistic effect existed between SPDV and MDH when applied in EVM matrix.

Cone calorimeter investigations based on the oxygen consumption principle could be used as a universal approach for ranking and comparing the fire behavior of materials. Therefore, it was not surprising that the cone calorimeter was finding increasing implementation as a characterization tool in the research and development of fire retarded polymeric materials.[34–36] Actually, the heat release rate (HRR) was one of most important parameters, and can be used to express the intensity of a fire. A highly flame retardant system normally showed a low HRR value. In this research, cone calorimeter experimental results for all the samples at a flux of 35 kW/m^2 were shown in Figures 4–Figure 8 and Table II. Figure 4 showed the HRR curves of the EVM/MDH system without SPDV. From Figure 4 and Table II, it could be found that the HRR and peak HRR (PHRR) values reduced as the loading of MDH increased, and the reduction in PHRR compared to pure EVM was nearly 43.9%, 62.1%, and 77.1% for EVM-2, EVM-3, and EVM-4, respectively. Moreover, compared with virgin EVM matrix, the time to ignition (TTI), fire performance index (FPI) and char residue increased, and the average HRR (AHRR), total heat release (THR) and average effective heat of combustion (AEHC) decreased for EVM-2, EVM-3, and EVM-4. Figure 5 showed the HRR curves of virgin EVM matrix and EVM/SPDV composite without

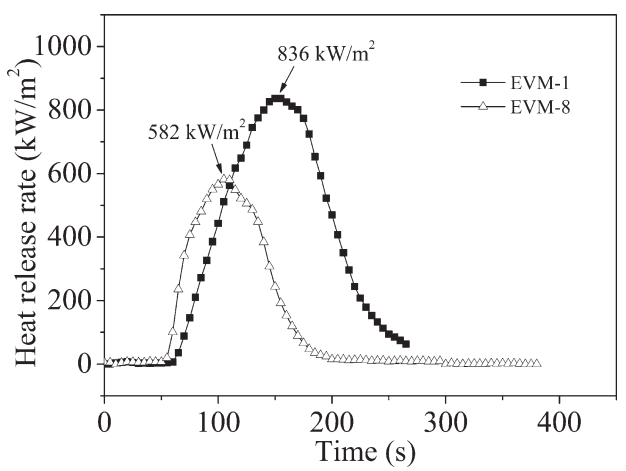

Figure 5 The HRR curves of virgin EVM matrix and EVM/SPDV composite without MDH.

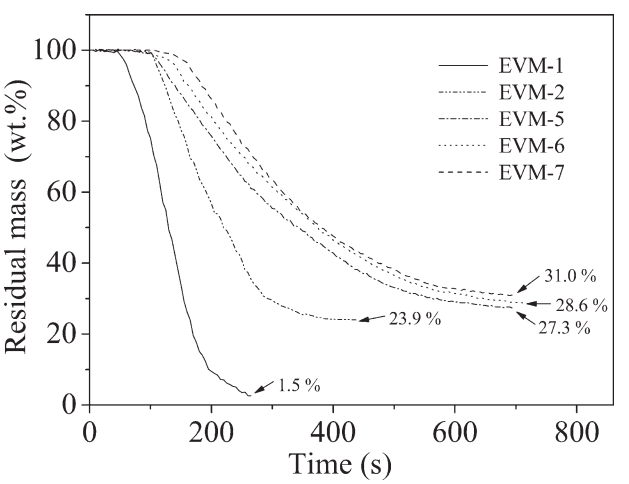

Figure 7 The residual mass curves versus burning time for the optimized EVM/MDH composites by SPDV.

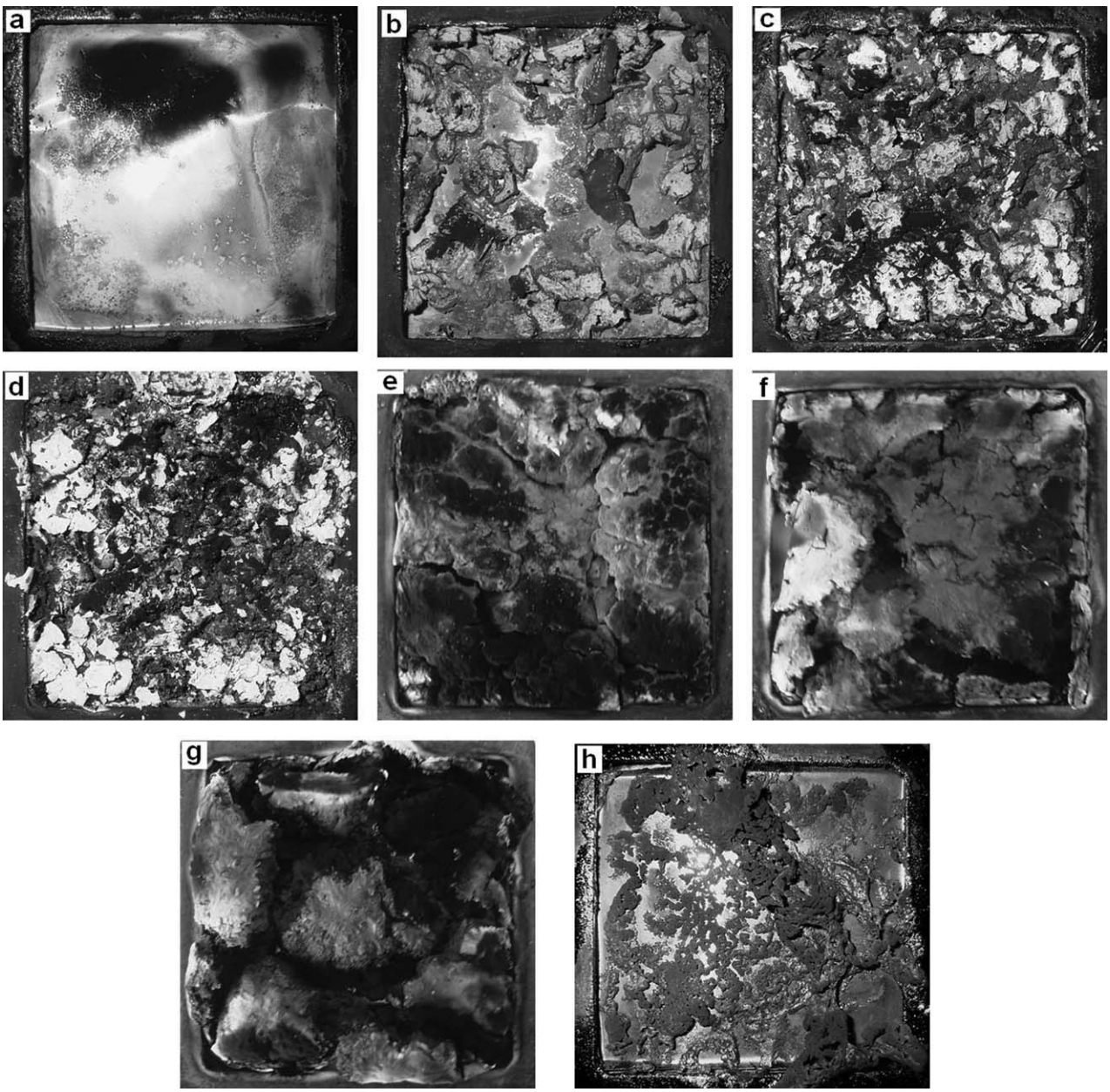

Figure 8 The residual images of virgin EVM matrix and flame-retardant EVM composites after combustion in cone calorimeter: (a) EVM-1; (b) EVM-2; (c) EVM-3; (d) EVM-4; (e) EVM-5; (f) EVM-6; (g) EVM-7; (h) EVM-8.

MDH. It could be found that the PHRR was reduced to 582 kW/m^2 for EVM-8 from 836 kW/m^2 for pure EVM matrix (EVM-1). Figures 6 and 7 showed the HRR and residual mass curves for the optimized EVM/MDH composites by SPDV. It could be found that the PHRR was reduced further for EVM-5, EVM-6, and EVM-7 compared with EVM-2, and the HRR curves became a sole peak while the sample EVM-2 presented two obvious peaks. Meanwhile, the burning time was further prolonged to higher than 700 s from less than 500 s for EVM-2. Compared with the EVM/MDH composite without SPDV (EVM-3, 317 kW/m^2), the optimized EVM/MDH composite by SPDV (EVM-7) presented a lower PHRR value (253 kW/m^2) with the same total amount of additives. From Figure 7 and Table II, it could be found that the residual mass was significantly increased for the optimized EVM/MDH composites, and the residual mass increased to 27.3%, 28.6%, and 31.0% for EVM-5, EVM-6 and EVM-7, respectively, while it was only 23.9% for EVM-2; the corresponding AHRR value decreased to 196, 175, and 163 kW/m^2 from 210 kW/m^2; the TTI changed to 96, 133, and 152 s from 97 s; the FPI increased to 0.279, 0.449, and 0.601 m^2·s/kW from 0.207 m^2·s/kW, respectively. All the above changes indicated that the flame retardancy was improved further for the optimized EVM/MDH composites by addition of

TABLE II
Cone Calorimeter Results of HFFR EVM/MDH Composites

Sample Code	TTI (s)	PHRR (kW/m^2)	AHRR (kW/m^2)	THR (MJ/m^2)	FPI (m^2·s/kW)	AEHC (MJ/kg)	Residues (%)
EVM-1	53	836	315	101	0.063	33.2	1.5
EVM-2	97	469	210	84	0.207	29.1	23.9
EVM-3	341	317	78	62	1.076	15.6	31.3
EVM-4	226	233	95	54	0.971	17.4	38.4
EVM-5	96	344	196	75	0.279	25.3	27.3
EVM-6	133	296	175	69	0.449	22.4	28.6
EVM-7	152	253	163	64	0.601	19.7	31.0
EVM-8	49	582	338	71	0.084	24.6	13.5

TTI, time to ignition; PHRR, peak of heat release rate, expressing the intensity of a fire; AHRR, average HRR within the front 400 s from heat radiation; FPI, fire performance index, the ratio of TTI and PHRR; AEHC, average effective heat of combustion.

SPDV. Figure 8(a–h) showed the residual images of virgin EVM matrix and flame-retardant EVM composites after combustion in cone calorimeter. It could be found that the pure EVM (EVM-1) had been burnt out and all the aluminum foil became visual, while the others for the flame-retardant EVM composites remained more or less residues and incumbent nearly or completely on the aluminum foil. Compared to the EVM/MDH composites without SPDV (EVM-2, EVM-3, and EVM-4) and EVM/SPDV composite without MDH (EVM-8), it could be found that the char residues presented intumescent behavior evidently for the optimized EVM/MDH composites by SPDV, and there was cracked and collapsed phenomenon for the char residues of EVM-6 and EVM-7 because of the dramatic expansion in combustion. Therefore, the synthesized SPDV had good flame retardant effect on the EVM/MDH composites, and a significant synergistic intumescent flame retardant effect existed between SPDV and MDH when applied in EVM matrix. Meanwhile, SPDV was both the char source and acidic source, and MDH was the gas source for intumescent flame retardant effect. Commonly, intumescent flame retardants could generate a swollen multicellular thermally stable char on heating which insulated the underlying material from the flame action and resulted in the extinguishment of combustion.[37,38] Moreover, compared with EVM/SPDV composite without MDH, the dispersed MDH in EVM matrix provided a mechanical strength to the whole compounds, and the increase of viscosity for the optimized EVM/MDH composites can better maintain the original shape without seepage of the melted polymer in combustion and improve the stability of the char layer, which was beneficial to reduce the transfer rate of volatile and play a more effective flame retardant effect for SPDV in solid state.

The thermal behavior of flame retardancy and FR-EVM composites

The fire performance of materials is closely associated with the thermal degradation of materials. TGA is one of the most favorite techniques for the rapid evaluation of the thermal stability of various flame retardant materials, and it indicates the decomposition of polymers at various temperatures. In this work, the thermal decomposition behavior of the flame retardancy and FR-EVM blends was studied by TGA. Figure 9 showed the TG (a) and DTG (b) curves of MDH, SPDV, and pure EVM matrix under air atmosphere. Obviously, it could be observed that MDH decomposes in one step, while SPDV in three steps. For the TG and DTG curves of MDH, the one-step decomposition in the range of 340–410°C was the dehydration reaction of MDH, and the residual mass at 800°C was about 69.7%. The initial decomposition temperature (IDT, defined as the temperature at which 5% weight loss of samples occurs) of SPDV was 245°C; those of pure EVM and MDH were 318°C and 366°C, respectively. Moreover, it can be interestingly seen that the synthesized SPDV presented very good charring ability and 44.6% of char residue remained at 800°C in air. This can be explained by the reason that the silicon-containing compounds degraded to generate silicon dioxide in air which couldn't be oxidized further and left in the char layer. The thermal stability of the char layer was further improved.

Figure 10 was the TG curves of the pure EVM (EVM-1) and optimized EVM/MDH composites by different loadings of SPDV (EVM-2, EVM-5, EVM-6, and EVM-7) under air atmosphere, respectively. From Figure 10, it can be seen that the pure EVM was thermally stable below 310°C and its thermal degradation occurred through a two-step weight loss. The first step was considered to involve the loss of acetic acid in the range of 320–380°C; the second was ranging from 410 to 500°C due to the degradation of carbon bone chain. The maximum mass loss rate of the first step was at 352°C and the second was at 445°C. Most of the mass loss of EVM matrix occurred in the second stage and only 1.4% residue existed at above 500°C. Compared with pure EVM, the optimized flame-retardant EVM/MDH

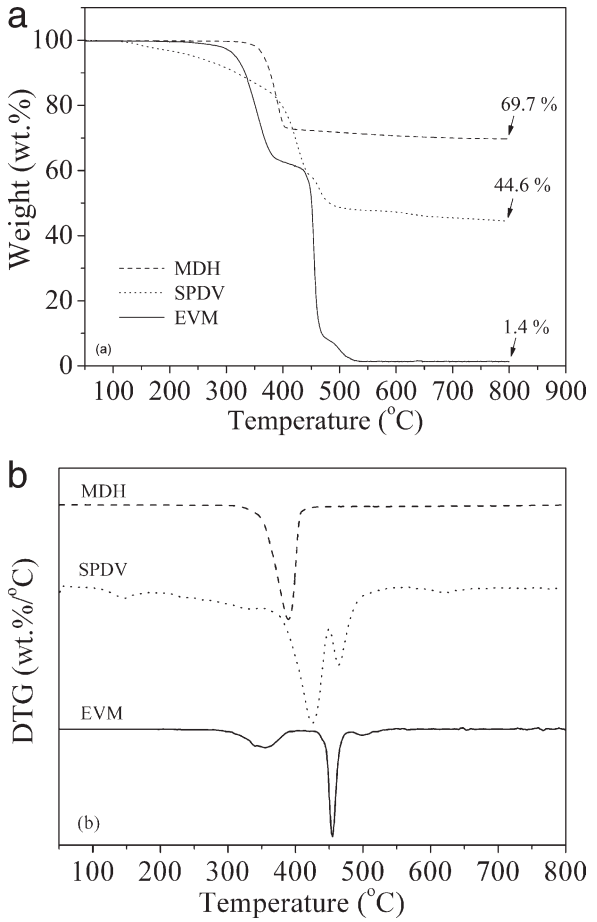

Figure 9 The TG (a) and DTG (b) curves of MDH, SPDV, and pure EVM matrix under air atmosphere.

composites had the similar thermal behavior with that of pure EVM at lower temperatures shown as Figure 10. It was noticed that the optimized flame-retardant EVM/MDH composites exhibited an enhanced thermal behavior at temperatures ranging

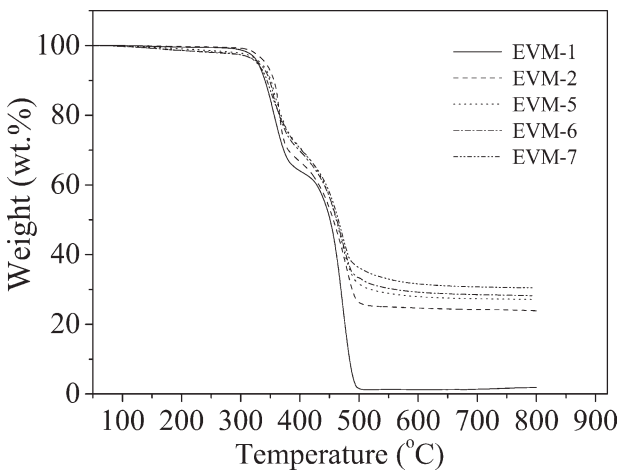

Figure 10 The TG curves of pure EVM and optimized EVM/MDH composites by different loadings of SPDV under air atmosphere.

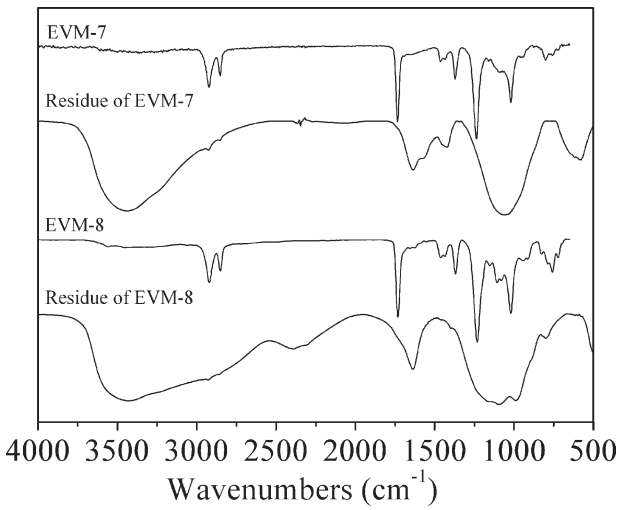

Figure 11 The FTIR spectrums of the EVM/SPDV composite (EVM-8) and the optimized flame-retardant EVM/MDH composite by SPDV (EVM-7) before combustion and the residue after cone calorimeter tests.

from 360 to 800°C, and presented a large amount of residue generated at 800°C. The yield of char residue at 800°C increased to 27.2%, 28.3%, and 30.5% for EVM-5, EVM-6, and EVM-7 as the loading of SPDV increased from 23.9% for EVM-2, respectively, which were higher than that of pure EVM (1.4%). This implied that SPDV and MDH could promote charring to form carbonaceous materials which could slow down heat and mass transfer between gas and condensed phases. Therefore, the flame retardancy of EVM was improved by addition of SPDV and MDH.

Chemical structural analysis of combustion residue by FTIR spectra

Figure 11 showed the FTIR spectrums of the optimized flame-retardant EVM/MDH composite by SPDV (EVM-7) and EVM/SPDV composite without MDH (EVM-8) before combustion and their residues after cone calorimeter test, respectively. From the spectrum of the residues for EVM-7 and EVM-8, it could be seen that the radical decrease of the typical absorptions of the acetic ester group (C═O, 1738 cm^{-1} and CH_3—C(═O)—, 1375 cm^{-1}) indicated the evolution of acetic acid, which was in agreement with the TG curves shown as Figure 10 (the first step of deacetylation reaction). The bands at 3480 cm^{-1} was assigned to the stretching mode of Si—OH or Mg—OH of residue remaining. The broad peaks at about 1000–1200 cm^{-1} may be the overlap for the stretching vibration of the P—O—C, P—O—P, P═O and Si—O—Si bond.[39–41] Based on the above, it could be concluded that a lot of phosphoric and silicic compounds were generated during the combustion. Meanwhile, it could be noticed that the bands at

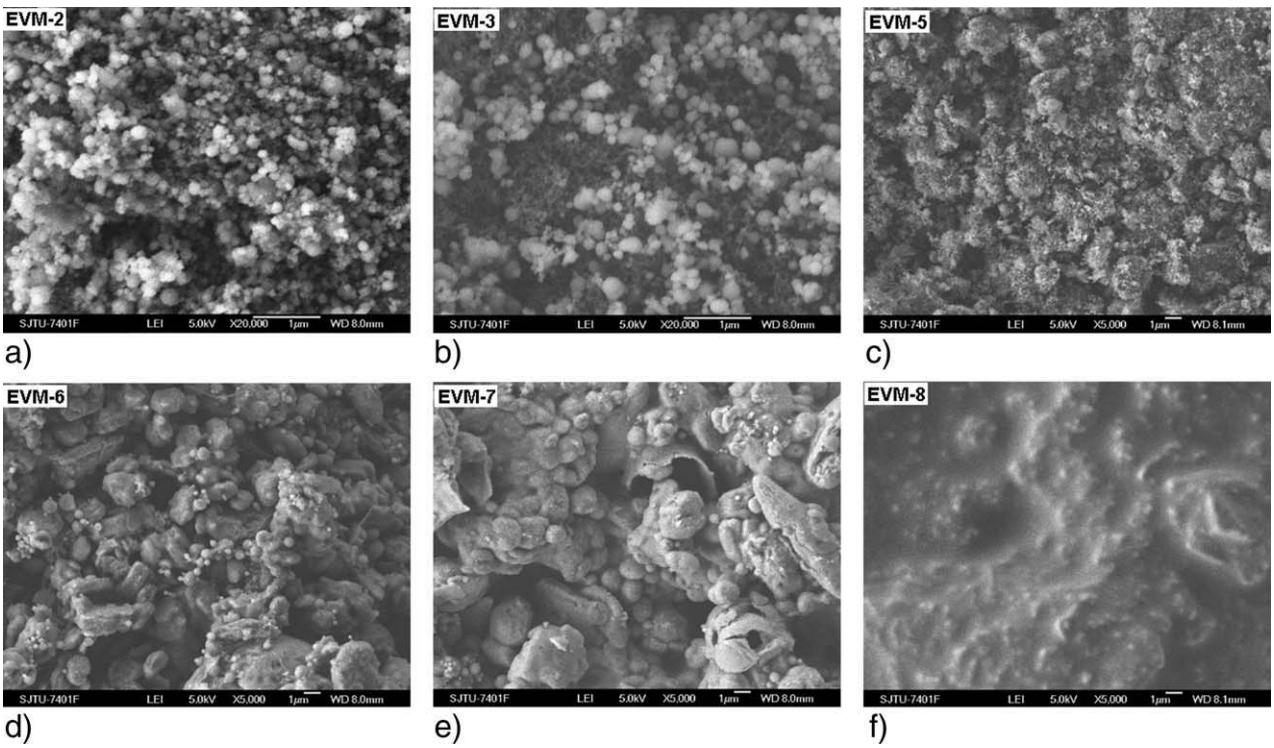

Figure 12 The microstructure of the residues after combustion in cone calorimeter tests for flame-retardant EVM samples: (a) EVM-2; (b) EVM-3; (c) EVM-5; (d) EVM-6; (e) EVM-7; (f) EVM-8.

1410 cm^{-1} was due to the organic part of the char and refer to the higher content of organic species in the residues for EVM-7 than EVM-8 because of the protection from MDH.[41]

Morphology of char residue by SEM

It was known that the effective protective char layer could improve the flame-retardant performance during combustion. To further investigate the effect of SPDV and MDH on the char formation of flame-retardant EVM composites during combustion, the morphologies of the chars were examined by SEM. SEM micrographs in Figure 12 showed the microstructure of the residue after combustion in cone calorimeter tests. Figure 12(a,b) showed the residual chars of EVM/MDH composites without SPDV filled with 50 and 80 phr MDH (EVM-2 and EVM-3), respectively. It could be found that there were many globular materials about hundreds of nanometers mainly composed of magnesia after combustion. Compared with Figure 12(a,b), it could be seen from Figure 12(c–e) that the residual char was more compact after combustion for the optimized EVM/MDH composites by SPDV (EVM-5, EVM-6, and EVM-7); and obviously, the residue of the optimized EVM/MDH systems had an intumescent structure and rich charred layers could be observed in the outer surface wrapping the magnesia. These provided a good barrier to the transfer of heat and mass during fire. Apparently, the intumescent char layer was the carbonaceous phosphorus-silicon-containing compounds by the SPDV after combustion shown as Figure 12(f).

Mechanical properties of FR-EVM composites

The mechanical properties of flame-retardant EVM-matrix composites were dependent on the flame-retardant additives and their dispersion state. Table III showed the mechanical test data for the different flame-retardant EVM-matrix materials. The stress–strain curves of EVM/MDH composites were similar in shape to those of the virgin EVM matrix, indicating that the presence of MDH did not modify the overall mechanical behavior of EVM matrix. Compared with virgin EVM, the tensile strength increased at beginning for the EVM/MDH composite with a

TABLE III
Mechanical Properties of Flame Retardant EVM/MDH Composites

Sample code	Stress at break (MPa)	Strain at break (%)
EVM-1	12.8 ± 1.2	552 ± 41
EVM-2	15.6 ± 0.8	516 ± 28
EVM-3	14.3 ± 0.6	479 ± 30
EVM-4	13.2 ± 0.7	386 ± 26
EVM-5	12.3 ± 1.0	473 ± 42
EVM-6	10.8 ± 1.1	437 ± 39
EVM-7	9.1 ± 0.7	389 ± 53
EVM-8	6.8 ± 0.9	432 ± 62

loading of 50 phr MDH (EVM-2), and then decreased while the loading of MDH was higher than 50 phr (EVM-3 and EVM-4). The tensile strength decreased for the optimized EVM/MDH composites with SPDV compared to EVM/MDH composites without SPDV, and the reason may be the lower compatibility between EVM matrix and the synthesized SPDV containing silicon. It was more evident for the reduction of tensile strength for EVM-8 shown as Table III. Compared to EVM/MDH composite without SPDV (EVM-4, 386 ± 26%), the optimized EVM/MDH composite with SPDV (EVM-6, 437 ± 39%) presented higher value of strain at break with the same vertical burning rating (V-0), and this was useful to the practical usage in wire and cable industry.

CONCLUSIONS

The flame retardant SPDV containing phosphorus and silicon was synthesized successfully and used for optimizing the FR properties of EVM/MDH composites. Compared with virgin EVM matrix, the FR performance was significantly improved for EVM/MDH composites. For the optimized EVM/MDH composites by SPDV, the FR performance was improved further due to the addition of SPDV. The results of cone calorimeter test showed that the HRR decreased and residual mass increased gradually as the loading of SPDV increased. The optimized formulation (EVM-6) was V-0 rating with the loading of 50 phr MDH and 20 phr SPDV, and presented higher value of strain at break than EVM-4. There existed distinct synergistic intumescent FR effect between SPDV and MDH in EVM matrix. TGA results showed that SPDV had good charring effect in air and the thermal stability was enhanced further for the optimized EVM/MDH composites by SPDV. The FTIR spectrums of char obtained from burning EVM/SPDV composites (EVM-7 and EVM-8) during cone calorimeter test suggested that a lot of phosphoric and silicic compounds were generated and high content of organic species still remained in the residues after the combustion. From SEM micrographs, rich char layers could be observed from the residues after combustion for the optimized EVM/MDH composites by SPDV, which was very useful to slow down heat and mass transfer between gas and condensed phases.

References

1. Chacko, A.; Sadiku, E. R.; Vorster, O. C. J Reinforced Plast Compos 2010, 29, 558.
2. Hausmann, K. Wire Cable Technol Int 2005, 34, 105.
3. Du, L. C.; Qu, B. J.; Xu, Z. J Polym Degrad Stab 2006, 91, 995.
4. Basfar, A. A.; Bae, H. J. J Fire Sci 2010, 28, 161.
5. Chen, T. Wire J Int 2005, 38, 57.
6. Fernandez, A. I.; Haurie, L.; Formosa, J.; Chimenos, J. M.; Antunes, M.; Velasco, J. I. Polym Degrad Stab 2009, 94, 57.
7. Beyer, G. Fire Mater 2005, 29, 61.
8. Hui, L.; Zhengping, F.; Mao, P.; Lie, S.; Yongchang, W. Radiat Phys Chem 2009, 78, 922.
9. Liang, J. Z.; Zhang, Y. J Polym Int 2010, 59, 539.
10. Marosfoi, B. B.; Garas, S.; Bodzay, B.; Zubonyai, F.; Marosi, G. Polymers Adv Technol 2008, 19, 693.
11. Ye, L.; Qu, B. J Polym Degrad Stab 2008, 93, 918.
12. Xie, F.; Wang, Y. Z.; Yang, B.; Liu, Y. Macromol Mater Eng 2006, 291, 247.
13. Zanetti, M. Polymer Nanocomposites; Woodhead Publishing Limited: Cambridge, 2006; p 256.
14. Jiao, C. M.; Wang, Z. Z.; Ye, Z.; Hu, Y.; Fan, W. C. J Fire Sci 2006, 24, 47.
15. Hirschler, M. M.; Piansay, T. Fire Materi 2007, 31, 373.
16. Morganl, A. B.; Cogent, J. M.; Opperman, R. S.; Harris, J. D. Fire Mater 2007, 31, 387.
17. Zhang, J.; Hereid, J.; Hagen, M.; Bakirtzis, D.; Delichatsios, M. A.; Fina, A.; Castrovinci, A.; Camino, G.; Samyn, F.; Bourbigot, S. Fire Safety J 2009, 44, 504.
18. Lv, J.; Qiu, L. Z.; Qu, B. J Nanotechnol 2004, 15, 1576.
19. Beyer, G. Fire Mater 2001, 25, 193.
20. Zhong, H. F.; Wu, D.; Wei, P.; Jiang, P. K.; Li, Q.; Hao, J. W. J Mater Sci 2007, 42, 10106.
21. Mosnacek, J.; Basfar, A. A.; Shukri, T. M.; Bahattab, M. A. Polym J 2008, 40, 460.
22. Nyambo, C.; Kandare, E.; Wilkie, C. A. Polym Degrad Stab 2009, 94, 513.
23. Li, Q.; Jiang, P. K.; Su, Z. P.; Wei, P.; Wang, G. L.; Tang, X. Z. J Appl Polym Sci 2005, 96, 854.
24. Zhong, H. F.; Wei, P.; Jiang, P. K.; Wu, D.; Wang, G. L. J Polym Sci Part B: Polym Phys 2007, 45, 1542.
25. Hermansson, A.; Hjertberg, T.; Sultan, B. A. Fire Mater 2005, 29, 407.
26. Li, Z. Z.; Qu, B. J Radiat Phys Chem 2004, 69, 137.
27. Rudi, R.; Orville, J. S. J Org Chem 1963, 28, 1608.
28. Wang, L. S.; Liu, Y.; Wang, R. J Chem Eng Data 2006, 51, 1686.
29. Zhong, H. F.; Wei, P.; Jiang, P. K.; Wang, G. L. Fire Mater 31, 411, 2007.
30. Enright, P. A.; Fleischmann, C. M. Fire Technol 1999, 35, 153.
31. Marney, D. C. O.; Russell, L. J.; Mann, R. Fire Mater 2008, 32, 357.
32. Schartel, B.; Bartholmai, M.; Knoll, U. Polym Degrad Stab 2005, 88, 540.
33. Carpenter, K.; Janssens, M. Fire Technol 2005, 41, 79.
34. Brohez, S. Fire Technol 2009, 45, 381.
35. Rychly, J.; Rychla, L. Polym Degrad Stab 1996, 54, 249.
36. Chow, W. K. J Fire Sci 2002, 20, 319.
37. Kandola, B. K.; Horrocks, A. R.; Horrocks, S. Fire Mater 2001, 25, 153.
38. Li, B.; Jia, H.; Guan, L. M.; Bing, B. C.; Dai, J. F. J Appl Polym Sci 2009, 114, 3626.
39. Wang, D. Y.; Cai, X. X.; Qu, M. H.; Liu, Y.; Wang, J. S.; Wang, Y. Z. Polym Degrad Stab 2008, 93, 2186.
40. Braun, U.; Balabanovich, A. I.; Schartel, B.; Knoll, U.; Artner, J.; Ciesielski, M.; Doring, M.; Perez, R.; Sandler, J. K. W.; Altstadt, V.; Hoffmann, T.; Pospiech, D. Polymer 2006, 47, 8495.
41. Camino, G.; Sgobbi, R.; Zaopo, A.; Colombier, S.; Scelza, C. Fire Mater 2000, 24, 85.